Soil and Soil Organic Carbon Effects on Simulated Southern High Plains Dryland Cotton Production

By

Steven A. Mauget[a]*, Sushil K. Himanshu[b], Tim S. Goebel[a], Srinivasalu Ale[b], Robert J. Lascano[a], Dennis C. Gitz III[a]

[a]Plant Stress and Water Conservation Laboratory, U.S. Department of Agriculture, Agricultural Research Service, Lubbock, TX, USA

[b]Texas A&M AgriLife Research (Texas A&M University System), Vernon, TX, USA

Submitted to *Soil and Tillage Research*

February 16, 2020

*Corresponding Author Address: 6926 Grover Ave. Lubbock, Texas, 79424. 1-806-698-6583, Steven.Mauget@.usda.gov

Keywords: Soil organic carbon, Pedotransfer functions, Soil water retention, Crop yield simulation, DSSAT, Conservation agriculture.

Abstract

The effect of increasing soil organic content (SOC) on the soil water retention and cotton yield productivity of two benchmark U.S. Southern High Plains (SHP) soils was estimated using pedotransfer functions and the CROPGRO-Cotton crop simulation model. Increasing plow layer (0-30 cm) SOC leads to increased wilting point (WP), field capacity (FC), and plant available water capacity (PAW = FC-WP) in both soils. The increase in a clay loam's available water capacity is modest, with a 1% increase in SOC producing an additional 0.16 cm of PAW in the soil profile's uppermost 30 cm. The fine sandy loam's plow layer effect is twice that, with a 1% SOC increase producing a 0.32 cm PAW increase. These effect's magnitudes were consistent with a recent meta-analysis of SOC on soil water retention, but considerably below those cited by national and regional extension services. As surface SOC levels in both soils were increased above baseline levels the fine sandy loam's median simulated cotton lint yields were essentially unchanged, while clay loam yields decreased. The clay loam yield effect is attributed to increased soil evaporation rates. Conservation agriculture (CA) practices such as increased residue retention may compensate for these weak soil water retention effects, but cotton's limited residue production would require winter cover crops or alternate crop rotations. As the success of terminated winter wheat – dryland cotton rotations is unclear in past SHP field studies, a CA sorghum-cotton rotation with periodic tillage is proposed as a SHP dryland production system.

1. Introduction

Despite the region's semi-arid climate, the Southern High Plains (SHP) of west Texas is the United States leading upland cotton (*Gossypium Hirsutum* L.) growing region, with 64% of planted cotton acres in un-irrigated 'dryland' production during 2012-2018 (NASS[1] 2019). As in any semi-arid growing region dominated by un-irrigated production, the area's yields are closely determined by rainfall variability. But in such water-limited agricultural areas soil water retention properties can also be important in determining how much rainfall ultimately becomes available to a crop's root-systems. The surface soils of the SHP were formed by wind-driven deposition that produced sandy soils in the southwest and soils with higher silt and clay content in the northeast (Holliday 1990). Decreased dryland cotton yields in the region's south relative to the north (Fig. 1) may be due in part to generally sandier soils with relatively limited water retention. As a result, attention has been drawn to management practices that might increase these soil's water retention, and, potentially, dryland yields.

Pittelkow et al. (2015) surveyed 678 studies that reported the effects of no-till cultivation within the set of practices known as conservation agriculture (CA), i.e., no or minimal soil disturbance, residue retention, and crop rotation. Their review found that, in contrast to wetter production environments, CA practices often either sustain or increase yields in dry climates. Among all the crop categories and locations they evaluated no-till reduced yields by 5.1%, but yields for cotton, oilseeds and legumes were not reduced. Lahmar's (2010) review of European CA adoption notes increased yields during drier years in semi-arid regions of Spain. In reviewing the results of 25 field experiments, Farooq et al. (2011) show evidence of positive yield effects of CA relative to conventional tillage in growing regions with less than 560 mm of annual rainfall.

[1] NASS: National Agricultural Statistics Service; SHP: Southern High Plains; WTM: West Texas Mesonet; AFSL: Amarillo Fine sandy Loam; PSCL: Pullman Silty Clay Loam; PTF: Pedotransfer Function; WP: Wilting Point; FC: Field Capacity; TRANS: Crop Transpiration; SEVAP: Soil Evaporation; SWCF: Final Column Soil Water Depth.

Page et al. (2020) summarized the reported effects of CA on increasing yields in drier climates and noted that many attributed those effects to increased soil water retention. Although Pittelkow et al. (2015) and Giller et al. (2009) note that applying CA in resource-poor settings may be difficult, these results suggest that it may be an effective approach to managing cotton in semi-arid dryland production.

In addition to reducing wind and water erosion, increasing water infiltration, improving soil quality, and increasing soil organic matter (Hobbs et al. 2008; Thierfelder and Wall 2009; Farooq et al. 2011; Serraj and Siddique 2012) CA practices may also have the potential of increasing soil water retention in the sandier soils of the SHP. Increases in soil organic matter (SOM) and carbon (SOC) lead to increased aggregate stability and decreased bulk density in a soil's surface layers, which can increase soil porosity and water retention (Huntington 2006; Blanco-Canqui and Benjamin 2013). Huntington (2006) and Rawls et al. (2003) demonstrate that increased SOC had greater effects on the volumetric water content (θ) at field capacity (θ_{fc}) relative to permanent wilting point (θ_{wp}), which would result in increased plant available water ($\theta_{paw} = \theta_{fc} - \theta_{wp}$). In addition, Rawls et al. (2003) found that those effects can vary with soil texture and the amount of SOC initially present in the soil. The increased water retention effects in coarse and sandier textured soils were found to be stronger than in fine-textured soils, and in the latter soils with high clay content the effect was reversed - increased SOC was found to decrease field capacity. The former effect is generally consistent with Minasny and Mcbratney's (2018; hereafter MM18) review of 60 globally published soil water retention studies, which indicated that the retention effects of an additional 1.0% of SOC were larger in sandy soils than in loams and clays.

The stronger water retention effects of increased SOC in sandier soils and potentially positive effects on cotton yields make conservation agriculture a promising approach to managing dryland SHP cotton production. Regional and national extension services suggest that the effects of increased SOC on water retention could be substantial. Based on the results of Emerson (1995), Mengel (2012) states that a 1% increase in SOM would result in an additional 187,058-223,823 L ha^{-1} (20,000-25,000 gallons $acre^{-1}$) of available soil water. Similarly, the U.S. Department of Agriculture's National Resource Conservation Service (NRCS 2013) claims that an additional 1% of SOM in the top 152 mm of soil would increase capacity by 252,529 L ha^{-1} (27,000 gallons $acre^{-1}$), or an equivalent water depth of 25.25 mm (.994 in). However, the MM18 meta-analysis indicates that these effects may be overstated. Based on the studies they reviewed, they estimate that a 1% mass increase in SOC produces average increases of saturation, field capacity, wilting point, and plant available water of, respectively, 2.95, 1.61, 0.17 and 1.16 mm of water per 100 mm of soil depth. But because soil organic carbon constitutes roughly half of soil organic matter by mass, a 1% SOM increase corresponds to a SOC increase less than 1.0%. Thus over a 152 mm soil depth a +1.0% SOM increase would result in less than an additional 1.76 mm (1.16 mm*1.52) of plant available water on average, considerably less than the 25.25 mm effect cited in NRCS (2013).

In previous work (Mauget et al. 2020) the DSSAT CROPGRO-Cotton crop model was used to generate cotton yields from the weather data of 21 West Texas Mesonet (WTM) stations (Fig. 1b) during a recent 11-year period. By converting the resulting 231 station-years of growing season weather outcomes into dense and climate-representative yield distributions, that simulation scheme was used to estimate yield and economic risk in SHP dryland cotton production. Here, a similar approach is taken to estimate the yield effects of varying soil type like those suggested by Fig. 1a, and of the water retention and yield effects of increasing SOC. Driving a crop model with data from multiple weather stations over multiple years provides two main advantages. First, unlike field studies that might be conducted under a limited number of years with unrepresentative seasonal weather conditions, it allows for generating dryland yields consistent with a much broader sampling of seasonal rainfall outcomes. Second, estimating SOC-related effects on water retention and yields through controlled field studies would be time and resource-intensive, as CA-related increases in the SOC of soil surface layers (Marland et al. 2003; Ogle et al. 2005; Govaerts et al. 2009) and agricultural yields (Farooq et al. 2011) may take decades to achieve.

The Mauget et al. (2020) simulations were conducted with a Pullman silty clay loam (fine, mixed, superactive, thermic Torrertic Paleustoll) that, according to Rawls et al.'s (2003) analyses, might be expected to have a relatively weak soil water retention response to increased SOC. To test the potentially stronger water retention response of the SHP region's sandier soils, the second soil type evaluated is an Amarillo fine sandy loam (Fine-loamy, mixed, superactive, thermic Aridic Paleustalf). The goals here are to: a) calculate and compare the soil water retention properties of both soils under baseline SOC levels, b) calculate those properties under increasing SOC conditions in the uppermost 30 cm both soils, and c), simulate the related effects on dryland cotton lint yields.

2. Methods

2.1 Soil core collection and analysis

Two 2.1 m soil cores were drawn from a Pullman silty clay loam soil (hereafter PSCL) soil at the USDA-ARS Bushland, TX location, and a pair of Amarillo fine sandy loam (hereafter AFSL) cores with the same depth were sampled at the ARS Lubbock, TX location. The PSCL and AFSL soil cores were collected using a tractor-mounted hydraulic soil sampler (Model GSRTS, Giddings Machine Sampler, Windsor CO). At each site the two 50-mm diameter soil cores were sampled less than 1.0 m apart. Each core was processed in the field by cutting them into 5 cm sub-samples to a depth of 0.3 m, 0.15-m samples to 0.6 m, and every 0.3-m down to 2.1 m depth for a total of 13 samples (Table 1).

One soil core for each soil was used for bulk density (BD) determination. Samples from both the AFSL and PSCL cores were collected in-house using a 53 mm X 50 mm soil sampling ring and sampling kit (Eijkelkamp, 2019). The soil sample rings were prepared as described in the Eijkelkamp user manual and placed into a sandbox (Eijkelkamp, 2019). The water level was raised to the appropriate level to saturate the samples and allowed to equilibrate for ten days until the weight of the rings stabilized. These samples were then oven dried and weighed again and BD was calculated.

The remaining soil core for each soil was used to estimate texture and SOC. The PSCL soil samples were analyzed in-house for particle size distribution of sand, silt and clay using oven-dried samples by the hydrometer method (Gee and Bauder, 1986). The AFSL soil samples were sent to the Texas A&M AgriLife Extension Service Soil, Water and Forage Testing Laboratory (SWFTL) for particle size analysis. The soil organic content of both soils was estimated at the SWFTL by the combustion method (McGeehan and Naylor 1988; Schulte and Hopkins 1996; Storer 1984).

2.2 Soil water retention calculation via pedotransfer functions

Pedotransfer functions (PTFs) can be used to estimate thermal, hydraulic, biogeochemical and gas exchange properties from a soil's structural and physical characteristics (Wösten et al.

2001; Van Looy et al. 2017). Although many of these properties can be measured in a laboratory, the time and expense required makes empirically derived functions more practical in many applications. These functions have been developed using a variety of methods, including regression trees (Rawls et al. 2003), power laws (Brooks and Corey 1964), logistic functions (Brutseart 1967; van Genuchten 1980) and neural networks (Schaap et al. 1998, 2001). But, as is typical with fitted functions, PTF accuracy can be reduced when used with a physical soil database different than that used to estimate the function's parameters (Schapp and Leij 1998; Guber et al. 2006). One approach to reducing this error is to use ensemble averaging, which averages the results from different PTFs to estimate the water retention properties common to all the PTFs. In addition, the variance in the individual PTF estimates can provide insight into the uncertainty of the ensemble averages. In some cases this approach may result in improved water retention estimates relative to laboratory-measured values. Based on a field experiment's soil and soil moisture data, Guber et al. (2006) conducted HYDRUS-1D simulations based on both PTF ensemble-estimated and laboratory-measured soil water retention properties. After comparing both sets of simulated soil moisture records with the experiment's time-domain reflectometer (TDR) measurements, they found that the simulations based on PTF-estimated soil parameters resulted in lower levels of validation error.

Although calculating PTF ensemble averages can involve different schemes for weighting individual functions (e.g., Guber et al. 2009), the approach here is a simple un-weighted averaging of PTF outputs similar to that of Guber et al. (2006). For both of the soils evaluated here, at each Table 1 sampling depth, the soil sample's volumetric water concentration at saturation (θ_s), field capacity (θ_{fc}), and permanent wilting point (θ_{wp}) was calculated using seven

PTFs (Table 2). Four of these functions calculate the parameters of the van Genuchten (1980) water retention equation based on Table 1's soil texture, BD, and SOC input values.

$$\frac{\theta(h) - \theta_r}{\theta_s - \theta_r} = \frac{1}{[1+(\alpha h)^n]^m} \quad (1)$$

where,

h is capillary pressure (cm),

$\theta(h)$ is the soil's volumetric water content ($cm^3\ cm^{-3}$) at capillary pressure h,

θ_r is residual volumetric water content ($cm^3\ cm^{-3}$),

θ_s is saturation volumetric water content ($cm^3\ cm^{-3}$),

α is a parameter approximately equal to the inverse of soil's air-entry pressure (cm^{-1}),

n is an estimated shape-defining parameter, and,

m = 1 -1/n

The PTF of Williams et al. (1992) calculated the parameters of the Brooks-Corey (Brooks and Corey, 1964) power relationship relating θ to h via:

$$\frac{\theta(h) - \theta_r}{\phi - \theta_r} = \left(\frac{h_b}{h}\right)^{\lambda} for\ h > h_b; 1\ for\ h \le h_b \quad (2)$$

where,

h_b is soil air entry pressure (cm),

ϕ is soil porosity ($cm^3\ cm^{-3}$), and,

λ is a pore size distribution index,

The Fortran subroutines for the van Genuchten and Brooks-Corey PTFs were selected from those in the CalcPTF pedotransfer function calculator (Guber and Pachepsky 2010) based on their use of SOC as an input variable. Using the PTF's estimated parameters and Eqs. 1 and 2, θ_{fc} and θ_{wp} values were calculated with capillary pressure values (h) corresponding to 33 and 1500 kPa. For soil saturation values derived from the Brooks-Corey equation, θ_s was approximated by 0.95*ϕ, as in Gijsman et al. (2002), and θ_r was set to 0.0. The Saxton and Rawls (2006) regression-based PTF calculates θ_{wp}, θ_{fc}, and θ_s directly from sand, clay, and SOC percentages. The Rawls et al. (2003) PTF similarly calculates θ_{wp}, and θ_{fc} from sand, clay and SOC content, with θ_s values estimated here as 95% of soil porosity. For both the Rawls et al. (2003) and Williams et al. (1992) PTFs soil porosity was calculated as 1.0 - BD/PD, as was θ_r in the Rawls et al. (1982) PTF. The required inputs for each PTF are listed in Table 2.

Saturated soil conductivity (K_{sat}) is a DSSAT input parameter that may be sensitive to SOC variation. Although the PTFs of Wösten et al. (1999), Saxton and Rawls (2006), and Weynants (2009) estimate K_{sat} based on SOC, the variability in those three K_{sat} estimates were found here to be wide enough to result in highly uncertain ensemble means. Based on that uncertainty, and that SOC effects on K_{sat} may be secondary to its effects on soil water retention (Blanco-Canqui and Benjamin 2013), K_{sat} values for the AFSL and PSCL soils were assigned at the Table 1 depths according to the values for Amarillo and Pullman soils reported by Baumhardt et al. (1995).

2.3 Estimating SOC effects on surface layer bulk density via regression.

Bulk density is a PTF and DSSAT soil input parameter that can be reduced by increased SOC levels (Chen et al. 1998; Rawls et al. 2003; Huntington 2006). Reduced BD can in turn increase soil porosity and θ_s in some of the Table 2 pedotransfer functions. Consistent with the Chen et al. (1998) and Rawls et al. (2003) meta-analyses, Table 1's measured SOC and BD values over both profiles are inversely proportional. In both soils SOC tends to decrease with depth while BD increases, most clearly in the 0–30 cm layers of the PSCL soil. As a result, the Table 1 baseline SOC and BD values are negatively correlated throughout the depth of both profiles, with the higher SOC-content PSCL soil showing stronger correlation (ρ= -.841) than the AFSL soil (ρ= -.537).

To account for the effects of varying SOC on BD in both soils, surface layer BD was estimated based on regression equations calculated by Chen et al. (1998). As management-related effects on SOC are generally considered to be limited to the top 30 cm of soil profiles (Mielke et al. 1986; West and Post 2002; Ogle et al. 2005,2012; Schwartz et al. 2015), surface layers were defined as Table 1's top 6 soil layers. Thus in the water retention estimates and DSSAT simulations each layer's BD below 30 cm is the Table 1 value. At and above 30 cm BD was estimated via Eqs. 3a-c, the layer's Table 1 clay and sand values, and variable SOC levels. For both soils, 0-30 cm SOC values were defined based on the Table 1 baseline levels, and by gradually increasing those levels to test the effects of increasing SOC on soil water retention and yields. Below 30 cm SOC levels were defined by the Table 1 values. Although Chen et al. (1998) calculated regressions for no-till and eight tillage implements, the Eqs. 3a-c regressions for the 0-10, 10-20, and 20-30 cm soil layers assume the use of disk plows commonly used in SHP cotton production.

$$\text{0-10 cm:} \quad BD = 1.373 - 0.447 * Clay + 0.141 * Sand - 0.0397 * SOM \qquad (3a)$$

$$\text{10-20 cm:} \quad BD = 1.568 - 0.538 * Clay - 0.0376 * SOM \qquad (3b)$$

$$\text{20-30 cm:} \quad BD = 1.682 - 0.732 * Clay \qquad (3c)$$

In Eqs. 3a-c clay is defined as clay fraction (0-1.0), sand as sand fraction (0-1.0), and the van Bemmelen SOC:SOM conversion factor (0.58) is assumed. Although Pribyl (2009) recommends a conversion factor of 0.5, a factor of 0.58 is used in these equations and in the Table 5 pedotransfer functions to maintain consistency with MM18.

2.4 Lint yield simulation via CROPGRO-Cotton

The Decision Support System for Agrotechnology Transfer (DSSAT) cropping system model (CSM: Jones et al. 2003; Hoogenboom et al. 2019) is an integrated collection of software components that includes separate modules to simulate the growth of individual crops, and soil-plant-atmosphere (SPAM), management, soil and weather modules common to the simulation of a range of crops. CROPGRO-Cotton (Pathak et al.,2007, 2012) is the DSSAT-CSM cotton growth module. The DSSAT SPAM module controls and regulates soil evaporation, plant transpiration, and root water uptake processes. The management module controls a simulation's management conditions, including; crop and cultivar selection, planting and harvesting dates, the timing of irrigation, fertilization, and tillage, and the application of chemicals, organic matter, residues, and chemicals. In addition to weather and management parameter inputs, the CSM requires species traits and cultivar characteristics, potentially variable CO_2 levels, and soil profile characteristics. DSSAT-CSM calculates and reports model state variables over daily time steps, although thermal time calculation and scaling of leaf to canopy assimilation is calculated hourly.

The weather module's daily weather inputs were calculated from weather data reported by the WTM network (Schroeder et al. 2005) at 5-minute intervals. For each of Fig. 1a's 21 mesonet stations, those 5-minute weather data records were used to identify daily maximum and minimum temperatures, and calculate daily average wind run and dew point temperature and total daily precipitation and solar radiation. This produced nearly continuous daily weather records for each station during Jan. 1 2005 to Dec. 31 2019, with data gaps filled-in with data from the station's nearest neighboring stations.

The DSSAT-CSM soil module computes soil temperature, soil water content, and soil nitrogen and carbon processes in up to 20 soil layers. The minimum required inputs include soil and location metadata, e.g., drainage, slope and soil surface albedo, and soil texture, BD and SOC levels. An internal PTF can calculate θ_{wp}, θ_{fc}, and θ_s based on texture, BD and SOC, but those θ values are superseded by externally input values as is done here. Water content for soil layers are updated daily using a one-dimensional tipping bucket water balance (Ritchie 1998; Boote et al. 2008) that regulates drainage and calculates each layer's water content between θ_{wp}, θ_{fc}, and θ_s. Drainage to lower layers occurs when soil water content is between θ_{fc} and θ_s, but soil θ can rise above θ_{fc} depending on the layer's K_{sat} value. Shelia et al. (2018) coupled the HYDRUS-1 hydrological model with the DSSAT-CSM and compared the resulting soil-water dynamics and crop simulation outcomes with those produced by field trial data and DSSAT's tipping bucket method. The tipping bucket approach produced lower RMS error between simulated and observed total soil water content, while its ability to reproduce biomass development in multi-year peanut and soybean field trials was comparable, and in some year's trial outcomes, better, than the Richards equation-based HYDRUS-1 method. Based on comparisons of simulated and observed soil water balances in field studies in the U.S., Spain, and Ghana, Boote et al. (2008) concluded that DSSAT's tipping bucket approach worked well if soil water retention, i.e., θ_{wp} and θ_{fc}, was properly defined, and if a crop's root growth was simulated properly.

The CROPGRO-Cotton simulations in this study used the Adhikari et al. (2016) cotton cultivar and ecotype parameters, which were estimated based on the 2010-2013 irrigated field trials described in Bordovsky et al. (2015). A summary of this calibration procedure can be found in Mauget et al. (2020), while Adhikari et al. (2016) provides a more detailed description. Each station-year's simulation began on May 1, with planting on May 15. The simulations assumed 76 cm rows with 3.0 plants per meter, resulting in a 39.5 K plants ha^{-1} plant density. Background soil nitrogen (N) was set to the regional average (96 kg ha^{-1}) estimated by Bronson et al. (2009), and no additional N was applied. As in Mauget et al. (2020) cotton lint yield is considered to be 39.1% of CROPGRO-Cotton's seed cotton output.

Daily weather input data from 21 WTM weather stations (Fig. 1a) during 2005-2010 and 2012-2019 were used to generate dryland lint yields representative of both soil's water retention properties under increasing SOC conditions. Although 2011 weather data was available, that year's unprecedented drought conditions (Hoerling et al. 2013) led to a complete failure of the west Texas dryland cotton crop. As the 2011 CROPGRO-Cotton simulations produced similar yield results, yields based on that year were not included in the aggregated yield distributions for each soil and SOC condition. Thus this process produced cotton lint yield distributions formed from yields derived from the daily weather inputs of each of the 294 (21*14) station-years.

The effect of SOC on each station-year's lint yield was simulated with different CROPGRO-Cotton input soil profiles as defined by the PTF ensemble averages of θ_{wp}, θ_{fc}, and θ_s, the Table

1 K_{sat} values, and the composite BD and SOC profiles described in Sections 2c. For both soils, different SOC profiles were formed based on the soil's Table 1 baseline SOC levels, and by increasing those levels in the 0-30 cm surface layers by equal ΔSOC increments. Hassink's (1997) analysis of the observed relationships between SOC and the silt and clay content of uncultivated and grassland soils in temperate and tropical regions suggests 6.0% as an approximate upper limit for SOC concentrations. Thus for both the PSCL and AFSL soils, nine SOC profiles were formed based on the soil's baseline SOC levels in Table 1, and by increasing those levels in the 0-30 cm surface layers by eight equal ΔSOC increments of 0.5%. As a result, for example, the highest 2.1% SOC level in the PSCL soil's top (0-5 cm) layer was increased by as much as 4.0%, resulting in a SOC level of 6.1%. Given the Table 2 texture inputs and the adjusted composite SOC and corresponding Eq. 3 BD profiles, θ_{wp}, θ_{fc}, and θ_s profiles were calculated from the outputs of the seven Table 2 PTFs. The CROPGRO-Cotton yield simulations were then based on the average of those θ profiles, and the composite SOC and BD profiles for that ΔSOC condition.

3. Results

3.1 Soil texture, organic carbon, and bulk density properties

Figures 2a and b plot Table 1's sand, silt, and clay profiles for the AFSL and PSCL soils. The most distinguishing textural characteristic between the two soils is the higher AFSL sand content. Above 30 cm AFSL sand varies between 68.5% and 80.0%, and below 30 cm never falls below 59.0%. Over the AFSL core's entire 210 cm depth silt content varies between 11.5 and 18.0%, while clay varies between 6.0 and 24.0%. By contrast, PSCL texture is more evenly divided between sand, silt, and clay throughout the profile depth. Above 30 cm, sand and silt content decrease with depth, while clay content increases. Below 30 cm, the average depth-weighted sand, silt, and clay contents are 20.3, 33.0, and 46.8% respectively.

Figures 2c plots both soil's measured (ΔSOC = 0%) organic carbon profiles over the cores's 210 cm depth. The PSCL SOC is uniformly higher, with the percentage in the highest (0-5 cm) layer (2.1%) almost 4 times that of the AFSL soil (0.54%). Figure 2d plots the BD profiles, which, again, are derived from Eqs. 3a-c at and above 30 cm, and are the measured Table 1 values in the seven layers below 30 cm. The solid traces in the 0-30 cm layers show the BD profiles under baseline SOC (ΔSOC = 0%) conditions. The dashed traces show the estimated effects of decreased BD due to a 4.0% SOC increase, and are limited to the 0-20 cm layers as SOC has no effect on BD in Eq. 3c. In the PSCL soil increased SOC causes average BD in the 0-20 cm layers to decrease 21.8% from 1.23 to 0.96 gm cm^{-3}. The effect in the AFSL soil is proportionately similar, with average 0-20 cm BD decreasing from 1.45 to 1.12 gm cm^{-3} (-22.7%).

3.2 Soil organic carbon effects on soil water retention

Figures 3a and b plot the θ_{wp}, θ_{fc} and θ_s outputs of the Table 2 PTFs for the AFSL and PSCL soils under baseline SOC conditions and the corresponding ensemble mean profiles. The PSCL θ_{wp}, and θ_{fc} mean profiles are clearly displaced towards higher volumetric water content relative to the AFSL profiles, with the PSCL ensemble-mean wilting points exceeding mean AFSL field capacity at each sampling depth. The 0.383 cm^3 cm^{-3} depth-weighted average of the PSCL ensemble-mean θ_{fc} over 0-210 cm is almost twice that of the AFSL soil (0.197 cm^3 cm^{-3}). Similarly, the 0-210 cm PSCL depth weighted average θ_{wp} (0.269 cm^3 cm^{-3}) is more than twice that of the AFSL soil (0.121 cm^3 cm^{-3}).

The solid traces of Figs 4a and b reproduce the θ_{wp}, θ_{fc}, and θ_s ensemble mean profiles of both soils in Figs. 3a, and b. The dashed traces show the corresponding profiles when the SOC inputs to the PTFs and Eqs. 3a-c in the 0-30 cm surface layers are increased 4.0 % above their Table 1 baseline SOC values. Table 3 shows the depth-weighted averages of θ_{wp}, θ_{fc}, and θ_s ensemble means over both soil's surface layers, e.g.,

$$\bar{\theta}_{fc} = \frac{1}{30\text{cm}} \sum_{i=1}^{6} \theta_{fc(i)} * \Delta Z_i \ , \qquad (4)$$

for the 0.0% to 4.0% ΔSOC levels. Figure 4's dashed profiles roughly follow their Fig. 3 baseline SOC counterparts above 30 cm, but are shifted towards higher θ values by varying degrees. In Fig. 4a and Table 3 the effect of raising AFSL surface SOC by 4.0% increases $\bar{\theta}_{wp}$ from 0.089 to 0.130, a 46.1% increase. Depth-weighted average AFSL field capacity ($\bar{\theta}_{fc}$) increases from 0.162 to 0.245, a 51.2% increase, while the surface layer's $\bar{\theta}_s$ increases by 17.9%. Although the PSCL soil has greater field capacity than the AFSL soil, the water retention effects of increasing SOC in Fig. 4b on wilting point and field capacity are proportionately smaller. A 4.0% increase in PSCL SOC results in 13.9% and 15.6% increases in $\bar{\theta}_{wp}$ and $\bar{\theta}_{fc}$ respectively. The +14.5% effect on PSCL surface $\bar{\theta}_s$ is more consistent with that found in the AFSL soil.

The PSCL soil has greater absolute water holding capacity due to its higher field capacity. However, the part of that capacity that is available to a crop's root system in both soil's surface layers is determined by the layer's plant available water capacity (PAW_s), i.e., the surface layer's total depth-weighted difference between θ_{fc} and θ_{wp}.

$$PAW_s = \sum_{i=1}^{6} \left(\theta_{fc(i)} - \theta_{wp(i)} \right) * \Delta Z_i \qquad (5)$$

The wider separation between θ_{fc} and θ_{wp} baseline values in the Fig. 3b PSCL 0-30 cm layers results in a PAW_s of 4.05 cm, while the AFSL soil's smaller θ_{fc} - θ_{wp} differences produce a PAW_s of 2.20 cm. Figure 4c shows the PAW_s values for both soils as ΔSOC is increased from 0 to 4.0% in 0.5% increments. Table 4 shows those values, and Table 3's corresponding depth-integrated values for wilting point (WP = 30 cm * $\bar{\theta}_{wp}$), field capacity (FC = 30 cm * $\bar{\theta}_{fc}$), and saturation (SAT = 30 cm * $\bar{\theta}_{s}$). In the AFSL soil a 4.0% SOC increase increases PAW_s 57.7% from 2.20 cm to 3.47 cm. In the PSCL soil that effect is proportionately smaller, with PAW_s increased from 4.05 cm to 4.78 cm (+18.1%). The proportional effects in Table 4 on WP, FC, and SAT are the same as those in Table 3 for $\bar{\theta}_{wp}$, $\bar{\theta}_{fc}$, and $\bar{\theta}_{fc}$ of both soils, which showed a stronger impact of increasing SOC on the wilting points and field capacities of the sandier AFSL soil's surface layers. But the proportionate effects of varying SOC in the 0-30 cm layers of both soils are much smaller when compared with the resulting changes in plant available water over the entire 0-210 cm soil profiles. Figure 4d graphs the total PSCL and AFSL plant available water (PAW_t) integrated over all 13 soil levels, i.e.,

$$PAW_t = \sum_{i=1}^{13} \left(\theta_{fc(i)} - \theta_{wp(i)} \right) * \Delta Z_i \ , \qquad (4)$$

as SOC in the surface layers is increased from 0.0% to 4.0% above baseline levels. In the AFSL soil PAW_t increases from 15.94 to 17.21cm (+8.0%), while PSCL PAW_t increases from 23.95 to 24.68 cm (+3.0%). Figures 4c and d also show the increased baseline water retention properties of the PSCL soil relative to the sandier AFSL soil. In Fig. 4c PSCL baseline PAW_s in the 0-30 cm layers (4.05 cm) is almost twice that of AFSL (2.20 cm) , while in Fig. 4d baseline PAW_t in the entire PSCL profile (23.95 cm) is 50.3% greater than that of AFSL (15.94 cm).

The MM18 meta-study reported estimates of the average effect of increased SOC on soil water retention through the changes in a 100 mm soil column caused by a 1% mass increase in SOC. Thus, for example, in Fig. 4c and Table 4 ΔSOC = +1.0% causes AFSL PAWs to increase from 2.20 to 2.52 cm over the depth of a 30 cm (300 mm) soil column. Scaling that 0.32 cm PAWs effect to a 100 mm soil depth and converting to millimeters results in an effect of 1.07 mm H_2O per 100 mm soil. Table 5 shows that ΔPAW/ΔSOC effect and the same effect calculated for the PSCL soil. In addition, similarly calculated effects for wilting point (ΔWP/ΔSOC), field capacity (ΔFC/ΔSOC), and saturation (ΔSAT/ΔSOC) are shown for both soils. For comparison, the corresponding average effects from MM18's meta-analysis of coarse, medium, and fine soil categories, and of all soils combined, are also included.

Based on the MM18 soil classification the AFSL soil is coarse-textured, while the PSCL soil is fine-textured. The effects of a ΔSOC = +1.0% increase on PSCL and AFSL PAW are well below the MM18 means for their respective soil classes, as are the effects on saturation. But, consistent with the greater MM18 average ΔPAW/ΔSOC effect in coarse soils relative to fine soils, the effect in the AFSL soil (1.07 mm) is about twice that of the PSCL soil (0.54 mm). The effects on AFSL (2.06 mm) and PSCL (1.39 mm) FC are comparable with the MM18 coarse (2.33 mm) and fine (1.28 mm) soil means, while the effect on AFSL (0.99 mm) and PSCL (0.85 mm) WP are greater than the MM18 coarse and fine soil averages. However, although the AFSL and PSCL responses in Table 5 clearly differ from their respective MM18 class averages in some cases, the four MM18 response parameters varied widely for some soil types and parameters (see MM18 Fig. 2).

But even after accounting for the MM18 variation in water retention responses, the most extreme are still considerably less than the effect suggested by NRCS (2013), i.e., that increasing SOM by 1.0% could increase soil water capacity by 25.25 mm in the uppermost 152 mm soil layer. The greatest average SOC effect shown in the MM18 meta-study was that of a saturation effect (ΔSAT/ΔSOC) in coarse soils of 4.59 mm H_2O 100 mm soil^{-1}, which when scaled to a 152 mm soil depth produces an additional saturation capacity of 6.98 mm H_2O. The most extreme effect in the MM18 response distributions is an approximately 9.0 mm H_2O 100 mm soil^{-1} saturation effect in coarse soils, which would produce an additional 13.68 mm H_2O in a 152 mm soil column. The MM18 water retention effects are associated with a +1.0% increase in SOC by mass. Assuming a 0.58 SOC:SOM ratio, water retention effects produced by 1.0% SOM increases are 58% of those than those produced by 1.0% SOC increases. Thus the most extreme +1.0% SOC water retention effect found in MM18 is well under half the 25.25 mm SOM effect proposed by NRCS(2013).

3.3 SOC effects on simulated dryland cotton lint yields

Figure 5a shows lint yield percentiles for dryland yields simulated with the AFSL and PSCL soils with baseline soil organic content, i.e., ΔSOC = 0.0, and distributions showing the lint yield effects of increasing ΔSOC by 0.5% to 4.0%. In these simulations the initial soil water at each of the 13 soil levels was set to field capacity under each SOC condition. As a result, they estimate yield effects generated from initial soil moisture conditions that track the increasing field capacity (Fig. 4a,b, Table 4) and plant available water (Fig. 4c,d) of each soil with increasing SOC. Figure 5b plots the medians of the corresponding Fig. 5a lint yield distributions.

In Fig. 5a the yield distributions for baseline SOC show lower yields in the AFSL soil, which is consistent with the general tendency for lower dryland yields in sandier SHP production areas

(Fig. 1). The AFSL and PSCL median simulated yields for ΔSOC = 0.0 are 303.4 and 482.1 kg ha^{-1} respectively. The AFSL median is below Fig. 1b's reported NASS District 12 median (383.0 kg ha^{-1}), while the PSCL median is fairly close to the District 11 median yield (490.6 kg ha^{-1}).

As SOC levels increase in the Fig. 5a AFSL yield simulations, the Fig. 5b median lint yields are basically unchanged, varying between 303.4 and 290.1 kg ha^{-1}. By contrast, median simulated PSCL yields decrease from 476.3 to 364.4 kg ha^{-1} (-23.5%) as ΔSOC is increased from 0.5% to 4.0%. Each station-year's PSCL simulations under both SOC levels were conducted with the same temperature and precipitation records, and only slightly different initial soil moisture when ΔSOC was increased from 0.0% (804.3 mm) to 4.0% (821.9 mm). Otherwise, the simulations were conducted identically except for the differences in 0-30 cm SOC and the related variation in BD, θ_{wp}, θ_{fc}, and θ_s. As a result, decreasing PCSL yields with increased SOC are likely due to shifts in water balances or soil properties in the simulation's surface soil layers.

The Fig. 6a scatterplot compares PSCL lint yields simulated under baseline SOC on the x-axis vs. the same station-year's yield simulated under ΔSOC = 4.0% soil conditions on the y-axis. Figure 6b's scatterplot similarly compares DSSAT-calculated total growing season crop transpiration (TRANS) under ΔSOC = 0.0% and 4.0% for each of the 294 station-years. Figure 6c compares final column soil water depth at the end of each simulation (SWCF), while Fig. 6d compares total growing season soil evaporation (SEVAP).

Increasing PCSL SOC by 4.0% in the top 30 cm of soil produces a median yield effect, i.e., the median of the vertical distances between each Fig. 6a data point and the figure's 1: l line, of – 113.4 kg ha^{-1}. Consistent with reduced yields, Fig. 6b shows reductions in total crop transpiration as SOC is increased, with a median effect of -11.6 mm. A scatterplot showing the effect of increasing SOC on cumulative growing season runoff are not plotted in Fig. 6, but shows scatterpoints along the 1:1 line with a negligible median effect (-0.11 mm). The effects of a 4.0% SOC increase on final soil water content in Fig. 6c are almost uniformly negative, with a median decrease in SWCF of -12.1 mm. This decrease occurs in spite of the ΔSOC = 4.0% PSCL simulations being initialized with 17.6 mm more soil column water than the baseline simulations. Unlike the remaining three scatterplots, Fig. 6d shows clearly increased soil evaporation, with a median growing season SEVAP effect of +40.9 mm. Thus the decreased PCSL yields as SOC is increased in Fig. 5 appear attributable to increased soil evaporation, decreased column soil moisture, and decreased transpiration.

4. Discussion

Increased SOC in both the PSCL and AFSL soil's 0-30 cm surface layers resulted in increased soil water retention in those layers, with stronger retention effects found in the sandier soil. Although the AFSL normally holds less water and is less productive than the PSCL soil, increased SOC led to proportionately larger increases in AFSL plant available water, field capacity, and wilting points (Tables 3,4). The stronger effects in the sandier AFSL soil are consistent with past studies of the effects of increased SOC on soil water retention (Rawls et al. 2003; Minasny and Mcbratney 2018). But although these effect's magnitudes were generally consistent with those of Minasny and Mcbratney's (2018) meta-analysis of the water retention effects of increased SOC (Table 5), they fell well below the effects claimed by regional (Mengel 2012) and national (NRCS 2013) extension services.

The claim that 1.0% of additional SOM can lead to increases of on the order of an additional 187,058 L ha^{-1} (20,000 gal ac^{-1}) of soil water capacity is found in extension literature (NRCS

2013; Mengel 2012; Bhadha et al. 2017), on the internet (Bryant 2015), and in the press (Goode, 2015). But although this common claim's origins are hard to trace, it may be based on an extreme estimate of the effects of SOM on soil water retention. The source reference cited by Mengel (2012) was Emerson (1995). Emerson's (1995) Table 2 shows the results of 7 studies that report a range of effects of increased SOC on plant available water (PAW) in various soil types. Those studies show effects from 1-10 grams of PAW increase for every 1 gram of SOC increase. The 10:1 effect reported by Salter and Haworth (1961) is arguably an outlier as the remaining 6 effects are in the range 1:1 to 4.9:1. If SOC = .58* SOM as is assumed here, a 10:1 PAW:SOC effect would correspond to a 5.8:1 PAW:SOM effect. However, Bryant (2015) estimates the effects of increased SOM on PAW based on a 10:1 PAW:SOM effect. That calculation assumes 1.33 g/cm^3 bulk density and concludes that a 1% SOM increase would result in an extra 202,658 L ha^{-1} (21,668 gal ac^{-1}) of PAW in the top 152 mm soil layers, which is consistent with the 187,058-223,823 L ha^{-1} effects cited by Mengel (2012). Thus both estimates appear to be based on an outlier 10:1 PAW:SOC water retention effect that also may not be accounting for the reduction of PAW_s:SOM effects relative to PAW_s:SOC effects. If the 4.9:1 PAW:SOC ratio in Emerson's (1995) Table 2 and a .58 SOC:SOM ratio are assumed, the resulting PAW:SOM effect is 2.8:1, which is more consistent with the theoretical effects in the 1.5:1 to 1.7:1 range calculated by Libohova et al. (2018).

In simulated crop production where initial soil moisture conditions tracked those of increasing field capacity as SOC was increased to 4.0% above baseline levels, median AFSL cotton lint yields were essentially unchanged, while median PSCL yields decreased (Fig. 5). Thus the proportionately greater water retention effects in the AFSL soil's surface layers had effectively no simulated yield impact. This may be due to the fact that, although SOC-related effects on water retention were restricted here to the 0-30 cm layers, the related plant available water capacity effects over the AFSL soil's total column depth (PAW_t) were proportionately much smaller (Fig. 4d). Thus the flat Fig. 5 AFSL yield effects suggest that management-related SOC increases in the surface layers of the SHP region's sandier soils may, by themselves, have limited yield effects. By contrast, increased 0-30 cm SOC led to positive but weaker PSCL soil water retention effects and a 24.1% reduction in median simulated yields when ΔSOC was raised to 4.0%. But although this extreme yield effect may be due to reduced transpiration and higher soil evaporation in the simulations (Fig. 6), the resulting PSCL SOC levels exceed values normally found in SHP Pullman soils. Schwartz et al.'s (2015) evaluation of the effects of tillage practices in a Pullman clay loam found surface SOC levels no higher than 3.4% in uncultivated soil (R. Schwartz personal communication). Although those observed grassland PSCL SOC levels may not represent saturated SOC conditions (Stewart et al. 2007), this suggests that the more extreme negative simulated PSCL yield effects found here might not be easily realized. Thus a shift to SOC levels consistent with current PSCL grassland conditions might produce a median yield effect more consistent with Fig. 5's ΔSOC=1.5% effect, i.e., a 7.1% drop from 482.1 kg ha^{-1} to 448.1 kg ha^{-1}.

The pedotransfer analyses here showed minor SOC-related increases in column-depth soil water retention in both soils. But because effects to plow depth (~30 cm) were assumed, even these modest effects may be liberal estimates compared to no-till practices. The effect of no-till was found to result in little or no SOC effect below 20 cm by West and Post (2002), and below 15 cm by Kern and Johnson (1993). But even with these liberal estimates, and contrary to the general conception of increased yields under conservation agricultural (CA) in drier conditions (Farooq et al. 2011; Pittelkow et al. 2015; Page et al. 2020), the associated crop simulations resulted in neutral or, under observed PSCL SOC conditions, mildly negative median yield effects.

Although CA practices may lead to effects from changes in tillage, residue retention, or crop rotation, only the effects of increased SOC on soil water retention and yields were tested here. Increased PSCL soil evaporation under higher SOC levels might be mitigated by residue retention, which has been associated with reduced evaporation and increased transpiration rates in irrigated SHP cotton field trails (Lascano et al. 1994; Baumhardt et al. 2013) and simulated dryland cotton soil water balances (Lascano and Baumhardt 1996). Thus a key CA practice that might compensate for the weak soil water retention effects found here may be the production and maintenance of residue cover. As cotton production provides relatively little residue (Bilbro and Fryrear 1985), mulching would likely be provided by a winter cover or alternate rotated summer crop. But in semi-arid rainfed agriculture, cover crops are generally considered to water-compete with the main cash crop and reduce yields (Dabney et al. 2001; Balkcom et al. 2007). Producing residue from terminated winter wheat in dryland SHP cotton field trials has resulted in no significant increase in water conservation or yields and made establishing cotton stands difficult (Baumhardt and Lascano 1999). Although Bordovsky et al.'s (1994) 1986-1989 SHP field trial found that a dryland cotton - terminated winter wheat crop rotation increased yields 12.6% relative to continuous cotton, those trials experienced above average May rainfall in each of the four years. The Baumhardt and Lascano (1999) field trials led them to recommend against a dryland cotton - winter wheat rotation. Conversely, without irrigation primary cash crops might water-compete with cover crops, leading to insufficient residue levels. Baudron et al.'s (2012) on-farm field experiments in Zimbabwe suggest that maintaining enough residue to improve infiltration and reduce runoff in sandier soils might be difficult in semi-arid dryland cotton production. Moreover, in semi-arid regions reduced tillage without sufficient residue cover can lead to soil degradation (Govaerts et al. 2009). Although increased residue and no-till practices might increase water infiltration, in semi-arid areas sandier soils that are susceptible to compaction and surface crusting can produce increased runoff, making periodic plowing necessary (Gerard 1986; Baudron et al. 2012).

5. Conclusions

In semi-arid dryland agriculture CA practices could in principle lead to a 'virtuous cycle' in increased soil organic content, increased soil water capacity, and increased biomass and yield production. Increased SOC levels might lead to increased field capacity and plant available water, which can in turn support increased biomass and yields. Increased biomass capacity might support the residue levels necessary to decrease runoff and evaporation and increase infiltration. Finally, the gradual transformation of increased surface biomass into soil carbon might complete the cycle by sustaining the trend towards increased SOC and plant available water.

But one link that makes this cycle possible, i.e., increased soil water capacity though increased SOC levels, was found to be weak in the two SHP soils tested here. This weak effect might be compensated for by the increased soil water inputs resulting from residue retention. However, the degree to which tillage and residue retention would counteract weak SOC-related soil water retention effects in past SHP field studies is unclear, as are the net effect of winter cover crops on dryland cotton yields and income. This uncertainty will be explored in future crop simulations of terminated winter wheat – dryland cotton rotations conducted under a range of seasonal climate and initial soil moisture conditions. But while winter cover crops might deplete soil moisture, increase production costs, and usually provide little or no income, sorghum is an

SHP dryland crop that might provide both residue and income. In addition, a sorghum-cotton rotation would allow for soil water recharge during winter fallow periods. As a result, sorghum-cotton rotations with cotton planted into the previous year's sorghum residues, with periodic tillage to address soil compaction as needed, might be considered as a dryland CA system in the SHP.

Acknowledgements

The authors would like to thank NOAA's National Mesonet Program and Texas Tech University for continued support in maintaining the West Texas Mesonet. Thanks to Lindsay Drunasky, Adam Wosoba, Jason Hardegree and Wil Hundl of the National Agricultural Statistics Service for help in obtaining cotton production data. All figures were produced using Generic Mapping Tools (Wessel et al. 2013). The mention of trade or manufacturer names is made for information only and does not imply an endorsement, recommendation, or exclusion by the USDA-Agricultural Research Service (ARS). This research was supported in part by the Ogallala Aquifer Program (OAP), a research consortium between the ARS and regional universities. The OAP played no role in study design, the collection, analysis and interpretation of data, the writing of the report, or the decision to submit the article for publication. The USDA is an equal opportunity provider and employer.

References

Adhikari, P., Ale, S., Bordovsky, J.P., Thorp, K.R., Modala, N.R., Rajan, N., Barnes, E.M., 2016. Simulating future climate change impacts on seed cotton yield in the Texas High

Plains using the CSM-CROPGRO-Cotton model. Agr. Water Manage. 164, 317–330. http://dx.doi.org/10.1016/j.agwat.2015.10.011.

Balkcom, K., Schomberg, H., Reeves, W., Clark, A., Baumhardt, L., Collins, H., Delgado, J., Duiker, S., Kaspar, T., and Mitchell, J., 2007. Managing cover crops in conservation tillage systems, in: Managing Cover Crops Profitably. Sustainable Agriculture Research and Education (SARE), College Park, MD, 44-61.

Baudron, F., Tittonell, P., Corbeels, M., Letourmy, P., Giller, K., 2012. Comparative performance of conservation agriculture and current smallholder farming practices in semi-arid Zimbabwe. Field Crop. Res. 132, 117-128. doi:10.1016/j.fcr.2011.09.008.

Baumhardt, R.L., Lascano, R.J., 1999. Water budget and yield of dryland cotton intercropped with terminated winter wheat. Agron. J. 91, 922–927. https://doi.org/10.2134/agronj1999.916922x.

Baumhardt, R.L., Schwartz, R., Howell, T., Evett, S.R., and Colaizzi, P., 2013. Residue management effects on water use and yield of deficit irrigated cotton. Agron. J. 105, 1026–1034. https://doi.org/10.2134/agronj2012.0361.

Baumhardt, R.L., Lascano, R.J., Krieg, D.R., 1995. Physical and hydraulic properties of a Pullman and Amarillo soil on the Texas South Plains. Texas A&M Agricultural Experiment Station at Lubbock/Halfway Technical Report 95-1, 20 pp.

Bhadha, J. H., Capasso, J. M., Khatiwada, R., Swanson, S., LaBorde, C., 2017. Raising soil organic matter content to improve water holding capacity. Publication #SL447. University of Florida IFAS Extension. Gainesville, FL. https://edis.ifas.ufl.edu/pdffiles/SS/SS66100.pdf (accessed 22 January 2021).

Bilbro, J.D., Fryrear, D.W., 1985. Effectiveness of residues from six crops for reducing wind erosion in a semiarid region. J. Soil Water Conserv. 40, 358–360.

Blanco-Canqui, H., Benjamin, J.G., 2013. Impacts of soil organic carbon on soil physical behavior, in: Logsdon S., Berli, M., and Horn, R. (Eds.), Quantifying and Modeling Soil Structure Dynamics, Vol. 3. ASA-CSSA-SSSA, Madison, WI., 11-40. https://doi.org/10.2134/advagricsystmodel3.c2.

Boote, K.J., Sau, F, Hoogenboom, G. and Jones, J.W., 2008. Experience with water balance, evapotranspiration, and predictions of water stress effects in the CROPGRO model., in: Ahuja, L.R., Reddy, V.R., Sassendran, S.A.,Yu., Q. (Eds.), Response of Crops to Limited Water: Understanding and Modelling Water Stress Effects on Plant Growth Processes. ASA - CSSA - SSSA, Madison, WI, 59-103. https://doi.org/10.2134/advagricsystmodel1.c3

Bordovsky, J.P., Mustian, J.T., Ritchie, G.L., Lewis, K.L., 2015. Cotton irrigation timing with variable seasonal irrigation capacities in the Texas south plains. Appl. Eng. Agric. 31, 883-897. https://doi.org/10.13031/aea.31.10953.

Bordovsky, J.P., Lyle, W.M., Keeling, J.W., 1994. Crop rotation and tillage effects on soil water and cotton yield. Agron. J. 86, 1–6. https://doi.org/10.2134/agronj1994.00021962008600010001x.

Bronson, K.R., Malapati,A. Booker, J.D., Scanlon, B.R., Hudnall, W.H., Schubert, A.M., 2009. Residual soil nitrate in irrigated Southern High Plains cotton fields and Ogallala groundwater nitrate. J. Soil Water Conserv. 64, 98–104. https://doi.org/10.2489/jswc.64.2.98.

Brooks, R. H., Corey, A.T., 1964. Hydraulic properties of porous media. Hydrol. Paper No. 3. Colorado State Univ., Fort Collins, CO. USA, 28 pp.

Brutsaert, W., 1967. Some methods of calculating unsaturated permeability. T. ASAE. 10, 400–404. https://doi.org/10.13031/2013.39683.

Bryant, L. 2015. “Organic Matter Can Improve Your Soil’s Water Holding Capacity.” National Resource Defense Council Expert Blog. https://www.nrdc.org/experts/lara-bryant/organic-matter-can-improve-your-soils-water-holding-capacity. (accessed 22 January 2021).

Chen, Y., Tessier, S., Rouffignat, J., 1998. Soil bulk density estimation for tillage systems and soil textures. T. ASAE. 41, 1606-1610. https://doi.org/10.13031/2013.17328.

Dabney, S.M., Delgado, J.A., Reeves, D.W., 2001. Using winter cover crops to improve soil and water quality. Commun. Soil Sci. Plan. 32, 1221–1250. https://doi.org/10.1081/css-100104110.

Eijkelkamp Soil & Water, 2019. Sandbox for pf-determination, M-0801E. Nijverheidsstraat, Netherlands. https://www.eijkelkamp.com/download.php?file=M0801e_Sandbox_for_pf_determination_d575.pdf (accessed 10 October 2020).

Emerson, W.W., 1995. Water-retention, organic-C and soil texture. Aus. J. Soil Res. 33, 241–251. https://doi.org/10.1071/sr9950241.

Farooq, M., Flower, K.C., Jabran, K., Wahid, A., Siddique, K.H.M., 2011. Crop yield and weed management in rainfed conservation agriculture. Soil Till. Res. 117,172–183. https://doi.org/10.1016/j.still.2011.10.001.

Gee, G., Bauder, J. 1986. Particle-size analysis. in: Klute, A., (Ed.), Methods of Soil Analysis. Part 4. 2nd ed. Agronomy Monograph No. 9. ASA-SSSA, Madison, WI., pp. 255-293.

Gerard, C.J., 1986. Laboratory experiments on the effects of antecedent moisture content and residue application on structural properties of a fragile soil. Soil Till. Res. 7, 63–74.

https://doi.org/10.1016/0167-1987(86)90008-5.

Gijsman, A.J., Jagtap, S.S., Jones, J.W., 2002. Wading through a swamp of complete confusion: how to choose a method for estimating soil water retention parameters for crop models. Eur. J. Agron. 18, 77–106. https://doi.org/10.1016/s1161-0301(02)00098-9.

Giller, K.E., Witter, E., Corbeels, M., Tittonell, P., 2009. Conservation agriculture and smallholder farming in Africa: the heretics' view. Field Crop. Res. 114, 23–34. https://doi.org/10.1016/j.fcr.2009.06.017.

Goode, E., 2015. 'Farmers Put Down the Plow for More Productive Soil'. New York Times, 9 March. https://www.nytimes.com/2015/03/10/science/farmers-put-down-the-plow-for-more-productive-soil.html. (accessed 21 January 2021).

Govaerts, B., Verhulst, N., Castellanos-Navarrete, A., Sayre, K.D., Dixon, J., Dendooven, L., 2009. Conservation agriculture and soil carbon sequestration: between myth and farmer reality. Crit. Rev. Plant Sci. 28, 97–122. https://doi.org/10.1080/07352680902776358.

Guber, A.K., Pachepsky, Y.A., van Genuchten, M.T., Rawls, W.J., Simunek, J., Jacques, D., Nicholson, T.J., Cady, R.E., 2006. Field-scale water flow simulations using ensembles of pedotransfer functions for soil water retention. Vadose Zone J. 5, 234–247. https://doi.org/10.2136/vzj2005.0111

Guber, A.K., Pachepsky, Y.A., van Genuchten, M.T., Simunek, J., Jacques, D., Nemes, A., Nicholson, T.J., Cady, R.E., 2009. Multimodel simulation of water flow in a field soil using pedotransfer functions. Vadose Zone J. 8, 1–10. https://doi.org/10.2136/vzj2007.0144.

Guber, A.K., and Pachepsky, Y.A., 2010. Multimodeling with Pedotransfer Functions. Documentation and User Manual for PTF Calculator (CalcPTF) Version 3.0.

https://www.ars.usda.gov/northeast-area/beltsville-md-barc/beltsville-agricultural-research-center/emfsl/docs/environmental-transport/calcptf/ (accessed 7 October 2020).

Gupta, S.C., Larson, W.E., 1979. Estimating soil water retention characteristics from particle size distribution, organic matter percent, and bulk density. Water Resour. Res. 15, 1633–1635. https://doi.org/10.1029/wr015i006p01633.

Hassink, J., 1997. The capacity of soils to preserve organic C and N by their association with clay and silt particles. Plant Soil. 191, 77-87. https://doi.org/10.1023/A:1004213929699.

Hobbs, P.R., Sayre, K., and Gupta, R., 2008. The role of conservation agriculture in sustainable agriculture. Philos. T. R. Soc. B. 363, 543–555. doi:10.1098/rstb.2007.2169.

Hoerling, M., Kumar, A., Dole, R., Nielsen-Gammon, J.W., Eischeid, J., Perlwitz, J., Quan, X.-W., Zhang, T., Pegion, P., Chen, M., 2013. Anatomy of an extreme event. J. Climate. 26, 2811–2832. https://doi.org/10.1175/JCLI-D-12-00270.1.

Holliday, V.T., 1990. Soils and landscape evolution of eolian plains: the Southern High Plains of Texas and New Mexico. Geomorphology. 3, 489–515. https://doi.org/10.1016/0169-555x(90)90018-l.

Hoogenboom, G., Porter, C.H., Boote, K.J., Shelia, V., Wilkens, P.W., Singh, U., White, J.W., Asseng, S., Lizaso, J.I., Moreno, L.P., Pavan, W., Ogoshi, R., Hunt, L.A., Tsuji, G.Y., Jones, J.W., 2019. The DSSAT crop modeling ecosystem, in: Boote, K.J., (Ed.), Advances in Crop Modeling for a Sustainable Agriculture. Burleigh Dodds Science Publishing, Cambridge, UK, 173-216. http://dx.doi.org/10.19103/AS.2019.0061.10.

Huntington, T.G., 2006. Available water capacity and soil organic matter. in: Encyclopedia of Soil Science. Taylor and Francis, New York, 139–143.

http://dx.doi.org/10.1081/E-ESS-120018496.

Jones, J.W., Hoogenboom, G., Porter, C.H., Boote, K.J., Batchelor, W.D., Hunt, L.A., Wilkens, P.W., Singh, U., Gijsman, A.J., Ritchie, J.T., 2003. The DSSAT cropping system model. Eur. J. Agron. 18, 235–265. http://dx.doi.org/10.1016/S1161-0301(02)00107-7.

Kern, J.S., Johnson, M.G., 1993. Conservation tillage impacts on national soil and atmospheric carbon levels. Soil Sci. Soc. Am. J. 57, 200–210. https://doi.org/10.2136/sssaj1993.03615995005700010036x.

Lahmar, R., 2010. Adoption of conservation agriculture in Europe: lessons of the KASSA project. Land Use Policy. 27, 4–10. doi:10.1016/j.landusepol.2008.02.001.

Lascano, R.J., Baumhardt, R.L., Hicks, S.K., Heilman, J.L., 1994. Soil and plant water evaporation from strip-tilled cotton: Measurement and simulation. Agron. J. 86, 987–994. https://doi.org/10.2134/agronj1994.00021962008600060011x.

Lascano, R.J., Baumhardt, R.L., 1996. Effects of crop residue on soil and plant water evaporation in a dryland cotton system. Theor. Appl. Climatol. 54, 69–84. https://doi.org/10.1007/bf00863560.

Libohova, Z., Seybold, C., Wysocki, D., Wills, S., Schoeneberger, P., Williams, C., Lindbo, D., Stott, D., Owens, P. R. 2018. Reevaluating the effects of soil organic matter and other properties on available water-holding capacity using the National Cooperative Soil Survey Characterization Database. J. Soil Water Conserv., 73, 411–421. https://doi.org/10.2489/jswc.73.4.411

McGeehan, S.L., Naylor D.V., 1988. Automated instrumental analysis of carbon and nitrogen in plant and soil samples. Commun. Soil Sci. Plant Anal. 19, 493-505. https://doi.org/10.1080/00103628809367953.

Marland, G., West, T.O., Schlamadinger, B., Canella, L., 2003. Managing soil organic carbon in agriculture: the net effect on greenhouse gas emissions. Tellus B. 55, 613–621. https://doi.org/10.1034/j.1600-0889.2003.00054.x.

Mauget, S., Marek, G., Adhikari, P., Leiker, G., Mahan, J., Payton, P., Ale, S., 2020. Optimizing dryland crop management to regional climate via simulation. Part I: US Southern High Plains cotton production. Front. Sustain. Food Syst. 3:120. doi: 10.3389/fsufs.2019.00120.

Mengel, D. 2012. The value of soil organic matter. in: Steve Watson (Ed.) Agronomy e—updates Number 357. Kansas State Extension Agronomy. Manhattan, KS. https://www.agronomy.k-state.edu/documents/eupdates/eupdate070612.pdf (accessed 8 October 2020).

Mielke, L.N., Doran, J.W., Richards, K.A., 1986. Physical environment near the surface of plowed and no-tilled soils. Soil Till. Res. 7, 355-366. https://doi.org/10.1016/0167-1987(86)90022-x.

Minasny, B., Mcbratney, A.B., 2018. Limited effect of organic matter on soil available water capacity. Eur. J. Soil Sci. 69, 39–47. https://doi.org/10.1111/ejss.12475.

NRCS (Natural Resources Conservation Service), 2013. Soil Health Key Points. https://www.nrcs.usda.gov/Internet/FSE_DOCUMENTS/stelprdb1082147.pdf (accessed October 8, 2020).

Ogle, S.M., Breidt, F.J., and Paustian, K., 2005. Agricultural management impacts on soil organic carbon storage under moist and dry climatic conditions of temperate and tropical regions. Biogeochemistry. 72, 87–121. https://doi.org/10.1007/s10533-004-0360-2.

Ogle, S.M., Swan, A., and Paustian, K., 2012. No-till management impacts on crop productivity, carbon input and soil carbon sequestration. Agr. Ecosyst. Environ. 149, 37–49.

https://doi.org/10.1016/j.agee.2011.12.010.

Page, K.L., Dang, Y.P., Dalal, R.C., 2020. The ability of conservation agriculture to conserve soil organic carbon and the subsequent impact on soil physical, chemical, and biological properties and yield. Front. Sustain. Food Syst. 4:31. doi: 10.3389/fsufs.2020.00031.

Pathak, T.B., Fraisse, C.W., Jones, J.W., Messina, C.D., and Hoogenboom, G., 2007. Use of global sensitivity analysis for CROPGRO cotton model development. T. ASABE. 50, 2295–2302. https://doi.org/10.13031/2013.24082.

Pathak, T.B., Jones, J.W., Fraisse, C.W., Wright, D., Hoogenboom, G., 2012. Uncertainty analysis and parameter estimation for the CSM-CROPGRO-Cotton Model. Agron. J. 104, 1363–1373. https://doi.org/10.2134/agronj2011.0349.

Pittelkow, C.M., Linquist, B.A., Lundy, M.E., Liang, X., van Groenigen, K.J., Lee, J., van Gestel, N., Six, J., Venterea, R.T., van Kessel, C., 2015. When does no-till yield more? A global meta-analysis. Field Crop. Res. 183, 156–168. https://doi.org/10.1016/j.fcr.2015.07.020.

Pribyl, D.W., 2010. A critical review of the conventional SOC to SOM conversion factor. Geoderma. 156:75-83. doi:10.1016/j.geoderma.2010.02.003.

Rawls, W.J., Brakensiek, D.L., Saxton, K.E., 1982. Estimation of soil water properties. T. ASAE. 25, 1316–1320. https://doi.org/10.13031/2013.33720.

Rawls, W.J., Brakensiek, D.L., Soni, B., 1983. Agricultural management effects on soil water processes part I: Soil water retention and Green and Ampt infiltration parameters. T. ASAE. 26, 1747–1752. https://doi.org/10.13031/2013.33837.

Rawls, W.J., Pachepsky, Y.A., Ritchie, J.C., Sobecki, T.M., Bloodworth, H., 2003. Effect of soil organic carbon on soil water retention. Geoderma. 116, 61–76.

https://doi.org/10.1016/s0016-7061(03)00094-6.

Ritchie, J.T., 1998. Soil water balance and plant water stress. in: Tsuji, G.K., Hoogenboom, G., Thronton, P.K. (Eds.), Understanding options for agricultural production. Kluwer Academic Publishers, Norwell, MA, 41-54. https://doi.org/10.1007/978-94-017-3624-4_3.

Salter, P. J., Haworth, F. 1961. The available-water capacity of a sandy loam soil. II. The effects of farmyard manure and different primary cultivations. J. Soil Sci. 12, 335-42. https://doi.org/10.1111/j.1365-2389.1961.tb00923.x

Saxton, K.E., Rawls, W.J., 2006. Soil water characteristic estimates by texture and organic matter for hydrologic solutions. Soil Sci. Soc. Am. J. 70, 1569–1578. https://doi.org/10.2136/sssaj2005.0117.

Schaap, M.G., Leij, F.J., 1998. Database-related accuracy and uncertainty of pedotransfer functions. Soil Sci. 163, 765–779. https://doi.org/10.1097/00010694-199810000-00001.

Schaap, M.G., Leij, F.J., Van Genuchten, M.T., 1998. Neural network analysis for hierarchical prediction of soil hydraulic properties. Soil Sci. Soc. Am. J. 62, 847–855. https://doi.org/10.2136/sssaj1998.03615995006200040001x.

Schaap, M.G., Leij, F.J., Van Genuchten, M.T., 2001. Rosetta: A computer program for estimating soil hydraulic parameters with hierarchical pedotransfer functions. J. Hydrol. 251, 163–176. https://doi.org/10.1016/s0022-1694(01)00466-8.

Schroeder, J.L., Burgett, W.S., Haynie, K.B., Sonmez, I., Skwira, G.D., Doggett, A.L., Lipe, J.W., 2005. The West Texas Mesonet: A technical overview. J. Atmos. Ocean. Tech. 22, 211–222. http://dx.doi.org/10.1175/JTECH-1690.1.

Schulte, E.E., Hopkins, B.G., 1996. Estimation of soil organic matter by weight Loss-On-Ignition. in: Magdoff, F.R., Tabatabai, M.A., Hanlon, E.A. Jr. (Eds.), Soil Organic matter: Analysis and Interpretation. Special publication No. 46. SSSA, Madison, WI., pp. 21-31. https://doi.org/10.2136/sssaspecpub46.c3.

Schwartz, R. C., Baumhardt, R. L., Scanlon, B. R., Bell, J. M., Davis, R. G., Ibragimov, N., Jones, O. R., Reedy, R. C., 2015. Long-term changes in soil organic carbon and nitrogen under semiarid tillage and cropping practices. Soil Sci. Soc. Am. J. 79, 1771-1781. doi:10.2136/sssaj2015.06.0241.

Serraj, R., Siddique, K., 2012. Conservation agriculture in dry areas. Field Crop. Res. 132, 1-6. doi:10.1016/j.fcr.2012.03.002.

Shelia, V., Šimůnek, J., Boote, K., and Hoogenboom, G., 2018. Coupling DSSAT and HYDRUS-1D for simulations of soil water dynamics in the soil-plant-atmosphere system. J. Hydrol. Hydromech. 66, 232–245. doi: 10.1515/johh-2017-0055.

Stewart, C. E., Paustian, K., Conant, R. T., Plante, A. F., and Six, J., 2007. Soil carbon saturation: concept, evidence and evaluation. Biogeochemistry. 86, 19-31. DOI 10.1007/s10533-007-9140-0.

Storer, D.A. 1984. A simple high volume ashing procedure for determining soil organic matter. Commun. Soil Sci. Plant Anal. 15, 759-772. https://doi.org/10.1080/00103628409367515.

Thierfelder, C., Wall, P.C., 2009. Effects of conservation agriculture techniques on infiltration and soil water content in Zambia and Zimbabwe. Soil Till. Res. 105, 217–227. doi:10.1016/j.still.2009.07.007.

van Genuchten, M.T., 1980. A closed-form equation for predicting the hydraulic conductivity of unsaturated soils. Soil Sci. Soc. Am. J. 44, 892–898.

https://doi.org/10.2136/sssaj1980.03615995004400050002x.

Van Looy, K., Bouma, J., Herbst, M., Koestel, J., Minasny, B., Mishra, U., Montzka, C., Nemes, A., Pachepsky, Y.A., Padarian, J., 2017. Pedotransfer functions in Earth system science: challenges and perspectives. Rev. Geophys. 55, 1199–1256. https://doi. org/10.1002/2017RG000581.

Wessel, P., Smith, W. H. F., Scharroo, R., Luis, J. F., Wobbe, F., 2013. Generic Mapping Tools: Improved version released. EOS Trans. AGU. 94, 409-410. https://doi.org/10.1002/2013eo450001.

West, T.O., Post, W.M., 2002. Soil organic carbon sequestration rates by tillage and crop rotation: a global data analysis. Soil Sci. Soc. Am. J. 66, 1930–1946. https://doi.org/10.3334/cdiac/tcm.002.

Weynants, M., Vereecken, H., Javaux, M., 2009. Revisiting Vereecken pedotransfer functions: Introducing a closed-form hydraulic model. Vadose Zone J. 8, 86–95. doi:10.2136/vzj2008.0062.

Williams, J., Ross, P., Bristow, K. 1992. Prediction of the Campbell water retention function from texture, structure, and organic matter. in: van Genuchten, M.Th., Leij, F.J., Lund, L.J. (Eds.), Proc. Int.Workshop on Indirect methods for Estimating the Hydraulic Properties of Unsaturated Soils. University of California, Riverside. pp 427-442. https://doi.org/10.13031/2013.39683.

Wösten, J.H.M., Lilly, A., Nemes, A., Le Bas, C., 1999. Development and use of a database of hydraulic properties of European soils. Geoderma. 90, 169–185. https://doi.org/10.1016/s0016-7061(98)00132-3.

Wösten, J.H.M., Pachepsky, Y.A., Rawls, W.J., 2001. Pedotransfer functions: bridging the gap between available basic soil data and missing soil hydraulic characteristics. J. Hydrol. 251, 123–150. https://doi.org/10.1016/s0022-1694(01)00464-4.

Figures

Figure 1. a) Percentiles of National Agricultural Statistics Service (NASS) districts 12 and 11 reported dryland lint yields over the 2012-2016 cropping years. b) Locations of 21 West Texas Mesonet (WTM) stations providing daily weather input data to the DSSAT CROPGRO-Cotton model during 2005-2019.

Figure 2. a) Sand, silt, and clay percentages at the 13 sampling levels for the AFSL soil. b) As in (a) for the PSCL soil. c) Soil organic carbon (SOC) percentage profiles for the AFSL and PSCL soils. d). As in (c) for bulk density (BD). BD values below 30 cm are Table 1 values, while values at and above 30 cm for both soils were determined by regressions from Chen et al. (1998). At and above 30 cm solid traces show BD values derived from Table 1 SOC values, dashed traces show BD profiles when SOC is raised by 4.0%. Below 30 cm both soil's BD profiles reflect Table 1 values.

Figure 3. a) AFSL volumetric water capacity at wilting point (θ_{wp}), field capacity (θ_{fc}), and saturation (θ_s). Small dots show Table 2 PTF outputs at each sampling levels, larger circles the level's ensemble mean. b) As in (a) for the PSCL θ_{wp}, θ_{fc}, and θ_s PTF outputs and ensemble means.

Figure 4. a) AFSL ensemble mean profiles of θ_{wp}, θ_{fc}, and θ_s under baseline SOC levels (solid trace), and when SOC is raised in the 0-30 cm levels by 4.0% (dashed traces). b) As in (a) for the PSCL baseline and ΔSOC = 4.0% ensemble mean profiles. c) Plant available water capacity for both soils integrated over the 0-30 cm levels under baseline and increased SOC levels. d) Plant

available water capacity for both soils integrated over the 0-210 cm levels under baseline and increased SOC levels.

Figure 5. a) Distributions of dryland lint yield simulated with AFSL and PSCL soils under baseline and increased soil organic content (SOC) levels. Initial soil moisture conditions at each soil level in the simulations were set to the field capacity of the corresponding soil type and SOC level. b) Median lint yields of the distributions for each soil type and SOC condition in (a).

Figure 6. a) Scatterplot of 294 PSCL lint yields simulated under baseline SOC conditions (x-axis) vs. the same station-year yield simulated under ΔSOC = 4.0% soil conditions (y-axis). b) As in (a) for total growing season transpiration (TRANS) simulated under baseline conditions vs. TRANS simulated under ΔSOC = 4.0% soil conditions. c) As in (a) for final soil water column depth (SWCF) simulated under baseline conditions vs. SWCF simulated under ΔSOC = 4.0% soil conditions. d) As in (a) for total growing season soil evaporation (SEVAP) simulated under baseline conditions vs. SEVAP simulated under ΔSOC = 4.0% soil conditions.

Tables

Table 1

				Amarillo Fine Sandy Loam						Pullman Silty Clay Loam				
Level	Depth (cm)	ΔZ (cm)		Sand (%)	Silt (%)	Clay (%)	SOC (%)	BD (gm/cm^3)		Sand (%)	Silt (%)	Clay (%)	SOC (%)	BD ($gm\ cm^{-3}$)
1	0-5	5		73	15	12	0.54	1.31		30	43	27	2.1	1.09
2	5-10	5		74	16	10	0.47	1.55		28	44	28	1.6	1.00
3	10-15	5		74	14	12	0.42	1.49		25.5	41.5	33	1.6	1.13
4	15-20	5		80	14	6	0.37	1.64		22	36	42	0.9	1.21
5	20-25	5		72	12	16	0.31	1.65		18.5	33.5	48	0.9	1.29
6	25-30	5		68.5	11.5	20	0.36	1.71		18	32	50	0.9	1.41
7	30-45	15		65	11	24	0.41	1.50		17.5	33.5	49	0.7	1.40
8	45-60	15		59	17	24	0.38	1.53		18.5	33.5	48	0.6	1.64
9	60-90	30		59	17	24	0.19	1.59		18	36	46	0.5	1.46
10	90-120	30		68	15	17	0.12	1.69		23	33	44	0.3	1.61
11	120-150	30		68	11	21	0.07	1.71		26.5	31.5	42	0.3	1.38
12	150-180	30		71	14	15	0.04	1.61		19	33	48	0.5	1.69
13	180-210	30		59	18	23	0.04	1.52		17	31	52	0.4	1.62

Table 1. Soil core sampling intervals, and the textural, soil organic carbon (SOC), and bulk density (BD) properties of the AFSL and PSCL soils.

Table 2

PTF	Region	Sand%	Silt%	Clay%	SOC%	BD	Method
Wösten et al. (1999)	Europe		X	X	X	X	VG
Rawls et al. (1982)	USA,nationwide	X	X	X	X	X	VG
Gupta and Larsen (1979)	Central USA	X	X	X	X	X	VG
Rawls et al. (1983)	USA,nationwide	X	X	X	X	X	VG
Williams et al. (1992)	Australia	X		X	X		BC
Saxton and Rawls (2006)	USA,nationwide	X		X	X		R
Rawls et al. (2003)	USA,nationwide	X		X	X		R

Table 2. The pedotransfer functions used here and their input requirements. Function methods include van Genuchten(VG), Brooks-Corey (BC), and regression (R).

Table 3

		Amarillo Fine Sandy Loam				Pullman Silty Clay Loam		
ΔSOC		$\bar{\theta}_{wp}$	$\bar{\theta}_{fc}$	$\bar{\theta}_{s}$		$\bar{\theta}_{wp}$	$\bar{\theta}_{fc}$	$\bar{\theta}_{s}$
0.0		0.089	0.162	0.424		0.244	0.379	0.512
+0.5		0.094	0.172	0.434		0.248	0.386	0.521
+1.0		0.099	0.183	0.443		0.252	0.393	0.530
+1.5		0.104	0.193	0.452		0.257	0.400	0.539
+2.0		0.109	0.204	0.462		0.261	0.407	0.548
+2.5		0.114	0.214	0.471		0.266	0.415	0.558
+3.0		0.119	0.225	0.481		0.270	0.422	0.567
+3.5		0.125	0.235	0.491		0.274	0.430	0.577
+4.0		0.130	0.245	0.500		0.278	0.438	0.586
		*46.1%	*51.2%	*17.9%		*13.9%	*15.6%	*14.5%

Table 3. Depth-weighted 0-30 cm averages of ensemble mean wilting point (θ_{wp}), field capacity (θ_{fc}), and saturation (θ_{s}) profiles for the AFSL and PSCL soils under increasing SOC levels. Starred values indicate the percentage increases caused by raising SOC in the 0-30 cm layers 4.0% above baseline (ΔSOC = 0.0%) levels.

Table 4

ΔSOC		Amarillo Fine Sandy Loam					Pullman Silty Clay Loam			
		WP	FC	SAT	PAW_s		WP	FC	SAT	PAW_s
0.0		2.67	4.87	12.73	2.20		7.32	11.36	15.36	4.05
+0.5		2.82	5.17	13.01	2.36		7.44	11.57	15.63	4.12
+1.0		2.97	5.49	13.29	2.52		7.57	11.78	15.90	4.21
+1.5		3.12	5.80	13.57	2.68		7.70	12.00	16.17	4.30
+2.0		3.27	6.12	13.86	2.84		7.83	12.22	16.45	4.39
+2.5		3.43	6.43	14.14	3.00		7.97	12.45	16.73	4.48
+3.0		3.58	6.74	14.43	3.16		8.10	12.67	17.02	4.58
+3.5		3.74	7.05	14.72	3.31		8.23	12.90	17.30	4.68
+4.0		3.90	7.36	15.01	3.47		8.36	13.13	17.69	4.78
					*57.7%%					*18.1%

Table 4. Depth-integrated wilting point (WP), field capacity (FC), saturation (SAT), and plant available water capacity (PAW_s) in centimeters for the AFSL and PSCL surface (0-30 cm) layers under increasing SOC levels. Starred values indicate the percentage increases in PAW_s caused by raising SOC 4.0% above baseline (ΔSOC = 0.0%) levels.

Table 5

Soil	ΔWP/ΔSOC	ΔFC/ΔSOC	ΔSAT/ΔSOC	ΔPAW/ΔSOC
AFSL	0.99	2.06	1.86	1.07
PSCL	0.85	1.39	1.79	0.54
MM18 Mean (Coarse)	0.86	2.33	4.59	1.94
MM18 Mean (Medium)	0.68	2.11	3.59	1.79
MM18 Mean (Fine)	0.54	1.28	3.23	1.41
MM18 Mean (All)	0.17	1.61	2.95	1.16

Table 5. Estimated rates of increase of volumetric water content (mm H_2O 100 mm^{-1} soil) over the AFSL and PSCL soil cores from a 1% increase in soil organic carbon (SOC). MM18 values show mean rates reported by Minasny and Mcbratney (2018) for coarse, medium, and fine soil categories, and all soil categories combined.

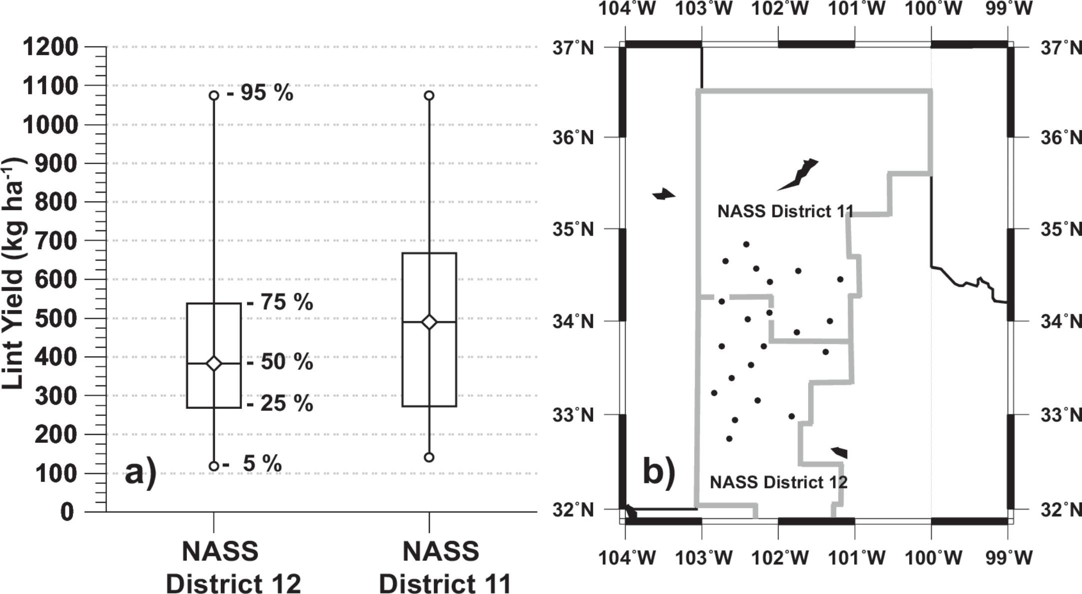

Lint Yield (kg ha-1)
1200
1100
1000
900
800
700
600
500
400
300
200
100
0
- 95 %
- 75 %
- 50 %
- 25 %
- 5 %
a)
NASS District 12
NASS District 11
104°W
103°W
102°W
101°W
100°W
99°W
37°N
36°N
35°N
34°N
33°N
32°N
NASS District 11
NASS District 12
b)

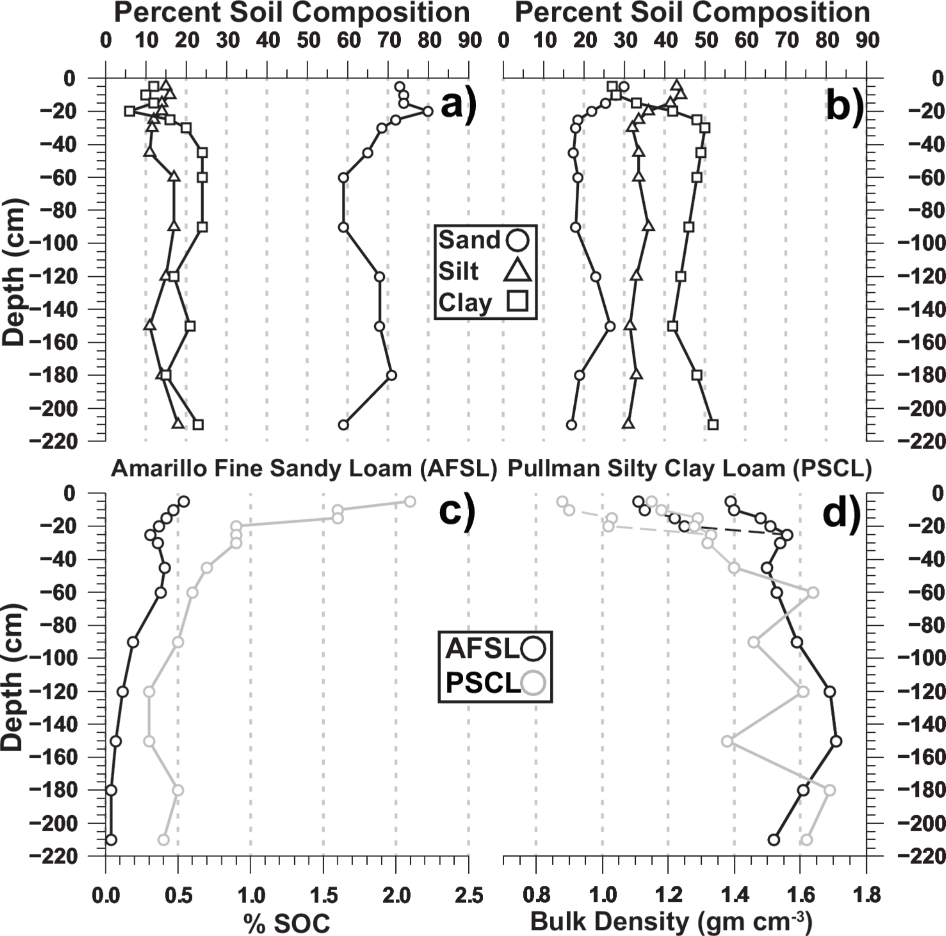

Percent Soil Composition
Percent Soil Composition
a)
b)
c)
d)
Sand
Silt
Clay
Depth (cm)
Amarillo Fine Sandy Loam (AFSL)
Pullman Silty Clay Loam (PSCL)
AFSL
PSCL
% SOC
Bulk Density (gm cm-3)

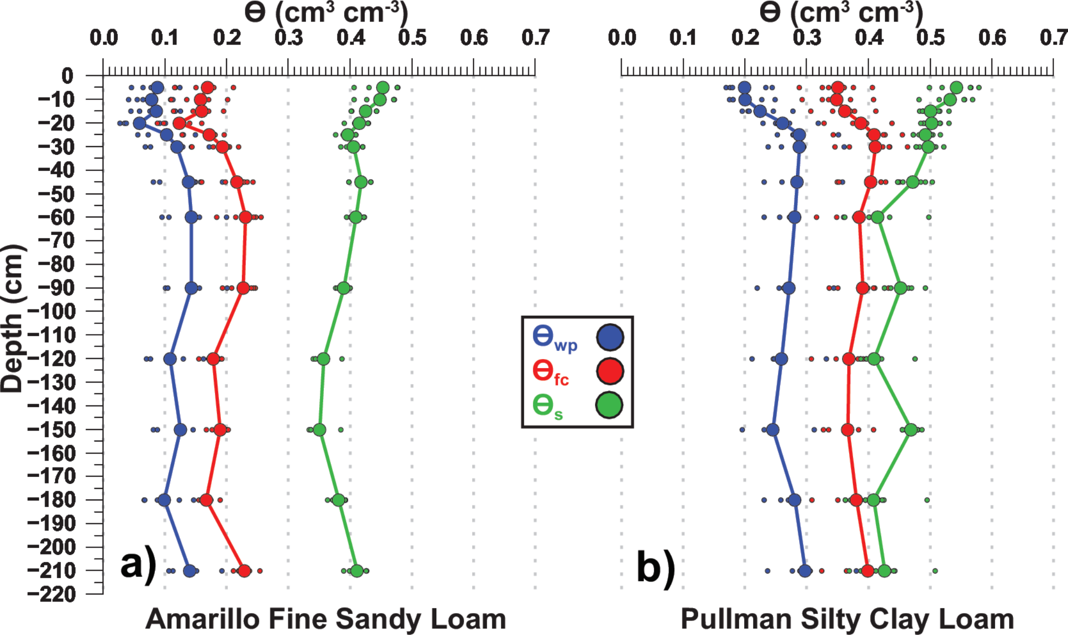

θ (cm³ cm⁻³)
0.0
0.1
0.2
0.3
0.4
0.5
0.6
0.7
Depth (cm)
0
−10
−20
−30
−40
−50
−60
−70
−80
−90
−100
−110
−120
−130
−140
−150
−160
−170
−180
−190
−200
−210
−220
a)
Amarillo Fine Sandy Loam
θ (cm³ cm⁻³)
0.0
0.1
0.2
0.3
0.4
0.5
0.6
0.7
b)
Pullman Silty Clay Loam
θwp
θfc
θs

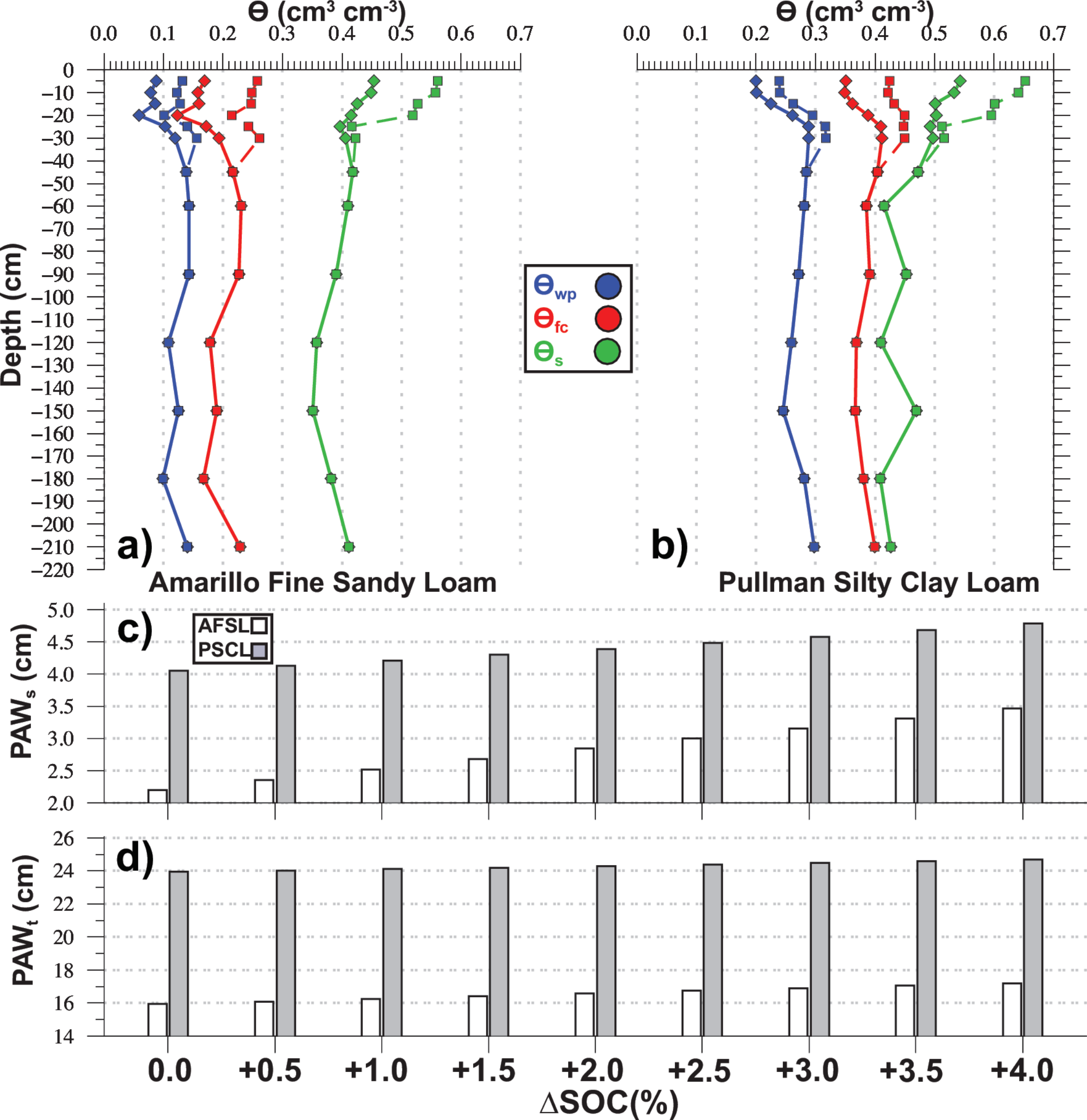

Θ (cm³ cm⁻³)
0.0 0.1 0.2 0.3 0.4 0.5 0.6 0.7
Depth (cm)
0 -10 -20 -30 -40 -50 -60 -70 -80 -90 -100 -110 -120 -130 -140 -150 -160 -170 -180 -190 -200 -210 -220
a)
Amarillo Fine Sandy Loam
b)
Pullman Silty Clay Loam
Θwp
Θfc
Θs
c)
AFSL
PSCL
PAWs (cm)
2.0 2.5 3.0 3.5 4.0 4.5 5.0
d)
PAWt (cm)
14 16 18 20 22 24 26
0.0 +0.5 +1.0 +1.5 +2.0 +2.5 +3.0 +3.5 +4.0
ΔSOC(%)

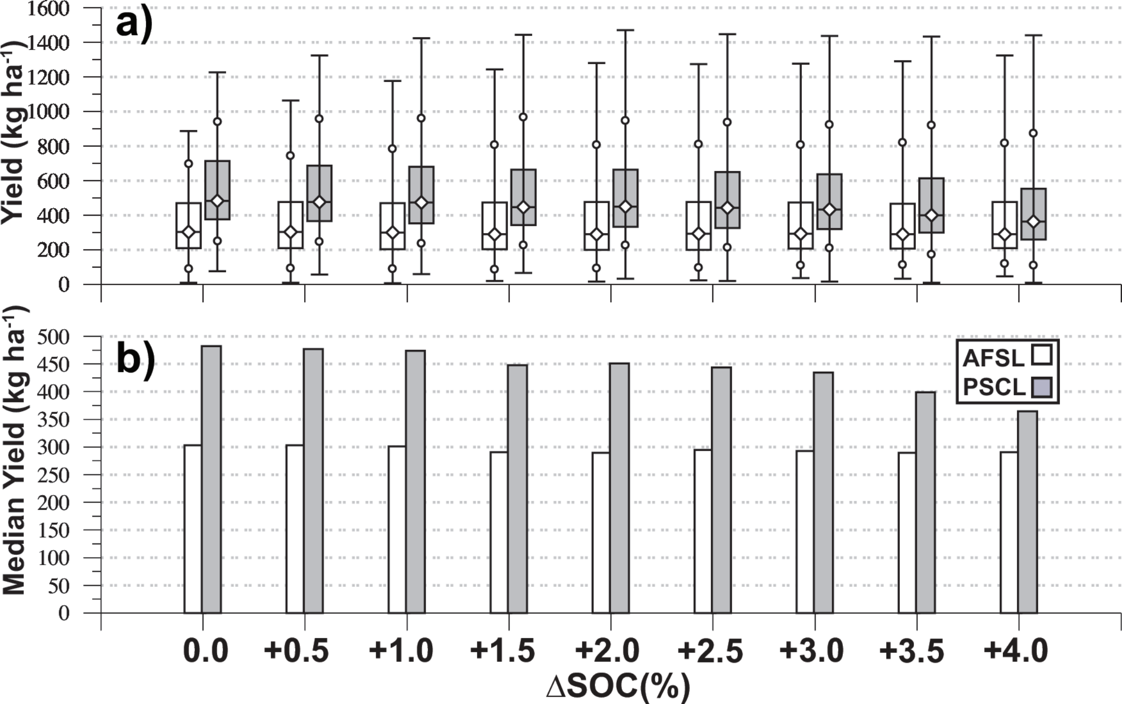

a)
b)
Yield (kg ha^{-1})
Median Yield (kg ha^{-1})
AFSL
PSCL
0.0
+0.5
+1.0
+1.5
+2.0
+2.5
+3.0
+3.5
+4.0
ΔSOC(%)

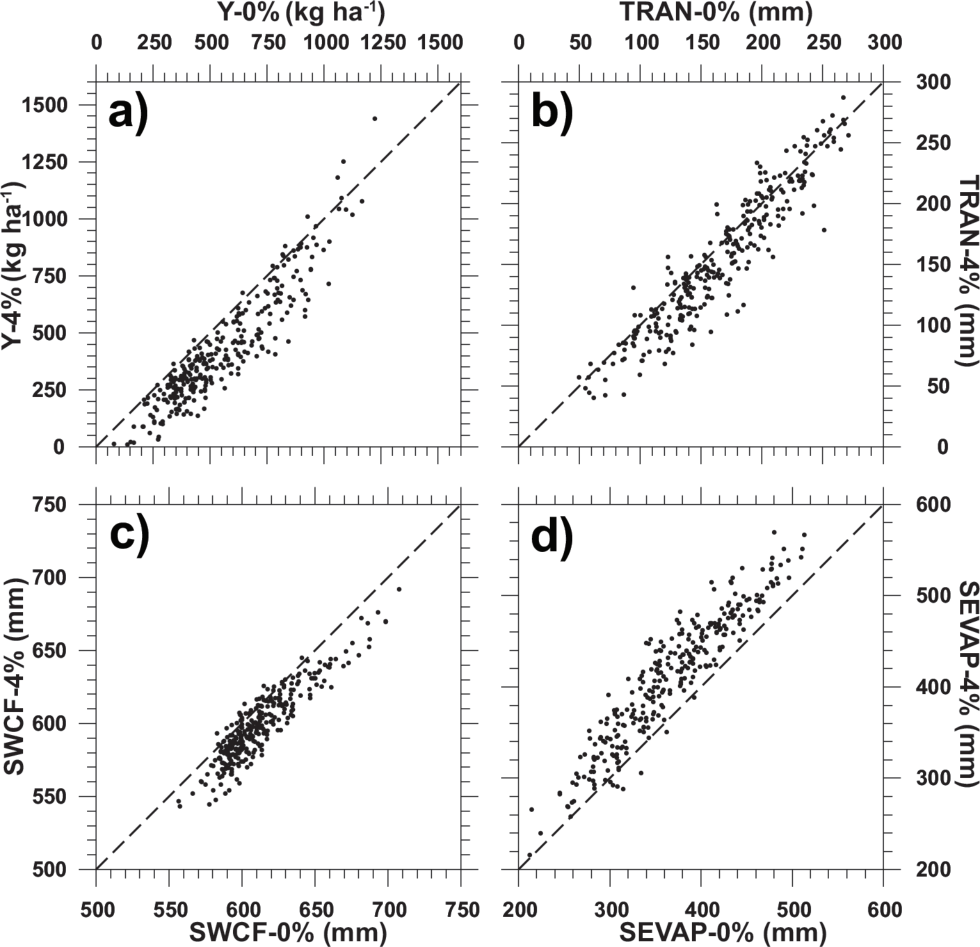

Y-0% (kg ha-1)
TRAN-0% (mm)
a)
b)
c)
d)
Y-4% (kg ha-1)
TRAN-4% (mm)
SWCF-4% (mm)
SEVAP-4% (mm)
SWCF-0% (mm)
SEVAP-0% (mm)
0
250
500
750
1000
1250
1500
50
100
150
200
300
400
550
600
650
700